Effect of changes in $\delta^{18}O$ content of the surface ocean on estimated sea surface temperatures in past warm climate

D. M. Roche,[1,2] Y. Donnadieu,[1] E. Pucéat,[1] and D. Paillard[1]

Received 14 September 2005; revised 27 January 2006; accepted 6 February 2006; published 29 June 2006.

[1] Using a coupled climate model of intermediate complexity including oxygen 18, CLIMBER-2, we investigate the evolution of the distribution of surface water ^{18}O composition under warm climate conditions. We then determine the impact of changes of the surface water ^{18}O distribution on ocean surface temperatures inferred from calcite oxygen 18. Our results show that published temperature reconstructions based on oxygen 18 from calcite are systematically biased by 2° to 4°C in the absence of major oceanic circulation changes and up to 7°C in the presence of major oceanic circulation changes. As the bias introduced is shown to vary with latitude, our work has major implications on past latitudinal temperature gradient reconstructions based on oxygen 18 measurements.

Citation: Roche, D. M., Y. Donnadieu, E. Pucéat, and D. Paillard (2006), Effect of changes in $\delta^{18}O$ content of the surface ocean on estimated sea surface temperatures in past warm climate, *Paleoceanography*, *21*, PA2023, doi:10.1029/2005PA001220.

1. Introduction

[2] The end of the Mesozoic and the beginning of the Cenozoic were punctuated by several intervals of markedly warm climates referred to as "greenhouse" climates (e.g., Turonian, early Eocene). One of the most problematic aspects of these periods is the apparent weak meridional temperature gradient. Temperature estimates, typically inferred from oxygen isotope composition of marine carbonate, indicate temperatures at high latitude up to 15°C warmer than at present but temperatures at low latitudes similar to those at present [*Pirrie and Marshall*, 1990; *Ditchfield et al.*, 1994; *Huber et al.*, 1995, 2002]. Although recent work suggests that some of the low-latitude estimates are too low [*Pearson et al.*, 2001; *Wilson and Norris*, 2001; *Norris et al.*, 2002; *Wilson et al.*, 2002], the inferred latitudinal temperature gradients are still weaker than the modern one [*Bice and Norris*, 2002; *Huber et al.*, 2002]. In models, increased atmospheric CO_2 levels are required to achieve the warm polar temperatures of past "greenhouse" climates. However, high atmospheric CO_2 levels cannot drive the weak temperature gradient, even after considering an absence of polar ice sheets. In order to reproduce weaker meridional temperature gradients, General Circulation Models need to assume an oceanic heat transport greater than present values [*Sloan et al.*, 1995; *Huber and Sloan*, 1999; *Bice and Norris*, 2002]. However, no satisfactory physical mechanism has been provided to support markedly enhanced poleward heat transport during warm periods [*Sloan et al.*, 1995; *Huber and Sloan*, 2001; *Pierrehumbert*, 2002], thereby questioning both the validity of climate models to reproduce past warm climates and our understanding of these periods.

[3] Most quantitative determinations of upper ocean paleotemperatures are derived from the oxygen isotope composition of planktonic foraminifera tests ($\delta^{18}O_{Ca}$), assuming that the carbonate was deposited in isotopic equilibrium with the surrounding waters. As the $\delta^{18}O_{Ca}$ records the evolution of both temperature and $\delta^{18}O$ of the water ($\delta^{18}O_{sw}$) surrounding the organism during calcite precipitation [*Epstein et al.*, 1953; *Shackleton*, 1974; *Erez and Luz*, 1983], assumptions are required on the latter to obtain temperature estimates. Although the mean $\delta^{18}O$ value of the global past ocean can be estimated with reasonable confidence for warm climates through the assumption of an "ice-free" Earth [*Shackleton and Kennett*, 1975], estimates of the latitudinal variations of $\delta^{18}O_{sw}$ are more uncertain. This knowledge is, however, critical to reconstruct past meridional temperature gradients from foraminiferal oxygen isotope compositions. Not accounting for this variation can bias the signal by several degrees [*Zachos and Stott*, 1994]. Still, there was little alternative but to suppose that the latitudinal distribution of the surface $\delta^{18}O_{sw}$ was the same in the past as at present day [*Crowley and Zachos*, 2000; *Bice and Norris*, 2002; *Zachos and Stott*, 1994].

[4] However, time intervals with warmer climates should have a stronger hydrological cycle with high precipitation rates at high latitudes. A correction can be made to account for this effect [*Manabe*, 1997]. In general, atmospheric general circulation models that incorporate stable isotope support higher $\delta^{18}O$ of precipitation ($\delta^{18}O_p$) at high latitudes during warm periods [*Jouzel et al.*, 2000]. Consequently, the latitudinal gradient of $\delta^{18}O_{sw}$ might be less than at present day [*Huber et al.*, 1995; *Bice and Norris*, 2002].

[1] Institut Pierre Simon Laplace/Laboratoire des Sciences du Climat et de l'Environnement, CEA-CNRS, Gif-sur-Yvette, France.

[2] Also at Department of Paleoclimatology and Geomorphology, Faculty of Earth and Life Sciences, Vrije Universiteit Amsterdam, Amsterdam, Netherlands.

0883-8305/06/2005PA001220$12.00

Therefore it was suggested to use a uniform $\delta^{18}O_{sw}$ and the present-day one to bracket the real warm climate $\delta^{18}O_{sw}$ distribution. However, changes in the surface $\delta^{18}O_{sw}$ latitudinal distribution not only depend on changes in $\delta^{18}O_p$ but also on changes in the net isotopic flux to the ocean [*Delaygue et al.*, 2000]. Let us consider the net isotopic flux from the atmosphere to the ocean written formally as follows:

$$F_{A\rightarrow O} = P\delta^{18}O_P - E\delta^{18}O_E \quad (1)$$

where P stands for precipitation, E for evaporation and $F_{A\rightarrow O}$ is the net atmosphere to ocean isotopic flux. From this formula, it is clear that a local drop in $\delta^{18}O_E$ (for example) could be compensated by an increase in the flux of evaporation, E. The aforementioned enrichment of $\delta^{18}O_p$ could then be counterbalanced by a higher water flux to the high-latitude oceanic surface water. In particular, an increased poleward latent heat transport (indicating a higher poleward moisture transport) has indeed been found in coupled simulations for the Eocene [*Pierrehumbert*, 2002]. Finally the surface latitudinal $\delta^{18}O_{sw}$ distribution also depends on the oceanic circulation which mixes water masses with different $\delta^{18}O_{sw}$. In particular, changes in zones and rates of deep convection can potentially have a strong effect on the $\delta^{18}O_{sw}$ of surface water in these regions.

[5] Changes in the latitudinal water transport and ocean circulation during past warm climates likely impacted the latitudinal distribution of surface water $\delta^{18}O$. In this study, we examine these effects using a couple ocean-atmosphere model.

2. Experiment's Definitions

[6] Here we explore the response of the latitudinal distribution of the $\delta^{18}O_{sw}$ to greenhouse conditions using a fully coupled ocean-atmosphere model, CLIMBER-2 [*Petoukhov et al.*, 2000], in a version including water isotopes [*Roche et al.*, 2004]. As described by *Roche et al.* [2004] water isotopes are not tracked explicitly in the atmosphere of the model, but simpler physical hypotheses have been made in order to evaluate the effect of atmospheric fractionation processes on the $\delta^{18}O$ of precipitation on a large scale. It has been shown that the isotopic module developed correctly simulates the present-day $\delta^{18}O_{sw}$ distribution. Furthermore, the computation of the isotopic fluxes being based on physical considerations solely, we are able to use this isotopic module under various climatic conditions, without any kind of external forcing or restoring conditions. Hence we are confident to use the model in the series of warm simulations proposed here.

[7] As our study is intended to demonstrate the overall effect of warmer climates on the $\delta^{18}O_{sw}$ latitudinal distribution we did not change the present-day geography to reproduce any particular period of time in the past. We only changed the external forcings in order to obtain different warm climates. The simulations are carried out with a present-day geography, starting from a preindustrial state and changing the solar constant to obtain a warmer climate. The different setups for the simulations are defined in Table 1, together with the labels used in the text.

Table 1. Parameters Used for Experiments' Definitions[a]

S, W m^2	pCO_2 Equivalent, ppm	ΔT, °C	Label in Text
1365	280	0	T0 (CTRL)
1400	840	+3.5	T3.5
1411	1120	+4.6	T4.6
1444	2240	+7.4	T7.4
1450	2520	+7.8	T7.8
1454	2800	+8.1	T8.1
1500	6720	+10.9	T10.9

[a]S is the solar constant, pCO_2 is the equivalent atmospheric carbon dioxide content according to *Kiehl and Dickinson* [1987], and ΔT is the increase in global average temperature with respect to the control run.

[8] The control run is a preindustrial one with pCO_2 = 280 p.p.m. For each modified solar constant, the model is then integrated until an equilibrium climate is reached. We chose to change the solar constant since the validity of the current CLIMBER-2 radiative code does not extend to very high levels of CO_2. For the simulations equivalent to moderate levels of CO_2, we also carried out simulations with CO_2 increase to check that the two methods yield the same results. We did not include the CO_2 simulations here, as they were almost identical to the modified solar constant ones.

[9] Since the isotopic fluxes at the ocean surface are simulated consistently with the climate, we are able to compute a simulated $\delta^{18}O$ of calcite from simulated $\delta^{18}O_{sw}$ and surface temperatures. That is, we use a rearrangement of the equation from *Shackleton* [1974] written as

$$\delta^{18}O_{Ca} = 21.9 + \delta^{18}O_{sw} - 0.27 - \sqrt{310.61 + 10T} \quad (2)$$

where T is the simulated water temperature and $\delta^{18}O_{sw}$ the simulated surface water isotopic content. This simulated $\delta^{18}O_{Ca}$ is, in turn, interpreted in terms of an isotopic temperature (labeled T*), assuming some a priori latitudinal $\delta^{18}O_{sw}$ distribution, as commonly applied to data. That is, T* is computed from [*Shackleton*, 1974]

$$T^* = 16.9 - 4.38\left(\delta^{18}O_{Ca} - \delta^{18}O_{sw}\right) + 0.1\left(\delta^{18}O_{Ca} - \delta^{18}O_{sw}\right)^2 \quad (3)$$

where $\delta^{18}O_{Ca}$ is the simulated isotopic content of the calcite and $\delta^{18}O_{sw}$ the assumed isotopic content of water, both in per mil (versus PDB and SMOW respectively).

[10] To evaluate the bias introduced by the use of this assumed surface water isotopic content, we distinguish two different $\delta^{18}O_{sw}$ latitudinal distributions from the literature. Indeed, the latitudinal $\delta^{18}O_{sw}$ profile is usually either taken constant or equal to the present-day one [*Sellwood et al.*, 1994; *Huber et al.*, 1995; *Crowley and Zachos*, 2000; *Bice and Norris*, 2002; *Pucéat et al.*, 2003], as two bracketing (extreme) hypotheses. When computing T*, the present-day latitudinal $\delta^{18}O_{sw}$ distribution of surface water is here the preindustrial simulated one, which has the advantage of being internally consistent with the simulated warm climate $\delta^{18}O_{sw}$. The difference between this temperature, T*, derived from the simulated calcite and the simulated water

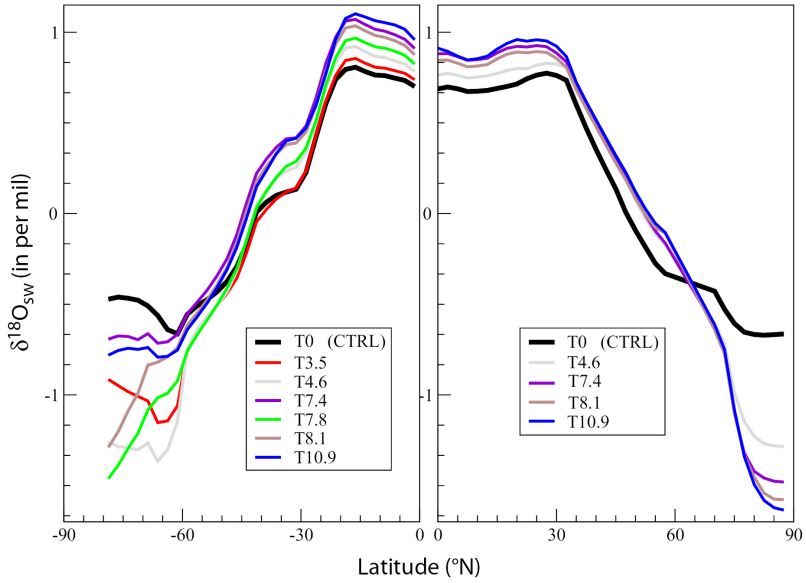

Figure 1. Changes in $\delta^{18}O_{sw}$ in warm climates. Figure 1 presents surface $\delta^{18}O_{sw}$ averages for the (left) Southern Hemisphere and (right) Northern Hemisphere of the CLIMBER model for the Atlantic and Pacific sectors. Black line shows the control simulation (preindustrial); colored lines show the warm climate simulations.

temperature, T, produced by the model therefore provides a quantitative measure of the systematic bias introduced using the assumed latitudinal $\delta^{18}O_{sw}$ distribution. In the following sections, we will use $T - T^*$ to quantify the error introduced using the classical $\delta^{18}O_{sw}$ latitudinal distributions described above.

3. The $\delta^{18}O_{sw}$ Latitudinal Distribution

[11] In our warm climate simulations, the surface $\delta^{18}O_{sw}$ of the ocean, presented in Figure 1, is higher than today in the tropical band and lower than today at high latitudes. The warmer the average climate becomes, the higher the differences are to a first order. They are due to a relatively simple phenomenon: As the climate gets warmer, there is increased humidity transport toward high latitudes. Since the exported humidity is depleted in $\delta^{18}O_{sw}$ with respect to surface oceanic waters, the net effect for the high-latitude ocean is a lower surface isotopic content. In other words, in spite of simulated less depleted high latitudes $\delta^{18}O_p$ (as in isotope-capable Atmospheric General Circulation Model [*Jouzel et al.*, 2000]), it appears that when considering a coupled climate model, the larger water fluxes provided to the high-latitude ocean in warm climates counterbalance the $\delta^{18}O_p$ enrichment in the determination of high-latitude $\delta^{18}O_{sw}$. For example, in the T3.5 (respectively T7.4) simulation, the simulated $\delta^{18}O_p$ increases by about 0.5–1‰ (respectively 0.5–1.5‰) with respect to the control for the 40 to 70° latitudinal band (north and south) and decreases by about 0–0.5‰ (respectively 0–0.5‰) in the intertropical regions on average. As deep waters are formed at high latitude, the overall isotopic content of the deep ocean decreases following the surface water. The total amount of isotopes in the earth system being constant, the intermediate depth and intertropical surface water's isotopic content increases relatively. This effect is referred to as the "compensation effect" in the following discussion.

[12] As temperatures derived from $\delta^{18}O_{Ca}$ are inversely related to the $\delta^{18}O_{sw}$, neglecting these changes leads to a temperature underestimation in the intertropical band and an overestimation at high latitudes. This is the opposite of what was usually assumed when considering only the high-latitude $\delta^{18}O_p$ enrichment without the "compensation effect" [*Bice and Norris*, 2002]. Furthermore, since this "compensation effect" depends on the relative volume of isotopically light deep waters versus heavier intermediate and surface tropical waters, the deep oceanic circulation is likely to affect the $\delta^{18}O_{sw}$ of surface water.

[13] From Figure 1, one can also infer that changes in the southern high-latitude surface $\delta^{18}O_{sw}$ are not linearly linked to the global mean temperatures. While T4.6 simulation still retains sea ice in this region, it completely disappears in simulations with higher global mean temperatures (T7.4, T7.8, T8.1 and T10.9). Although sea ice formation has little effect on the surface water $\delta^{18}O_{sw}$ [*Paren and Potter*, 1984], it is an important process for salinity and hence for vertical mixing, which bears the potential for modifying the $\delta^{18}O_{sw}$. As a consequence, the mode of Antarctic Bottom Water formation, which occurs in these regions, shifts from a present-day-like thermohaline type to a warm climate more thermal type. It does not mean that salinity has no role, but that because of the disappearance of sea ice, salinity gradients are less pronounced. Therefore thermal gradients tend to play the major role. Hence mixing is modified and consequently the $\delta^{18}O_{sw}$ of surface water as well.

[14] The changes in oceanic convection can be inferred from Figure 2 which shows the fraction of the year for which convection occurs for southern high latitudes. The

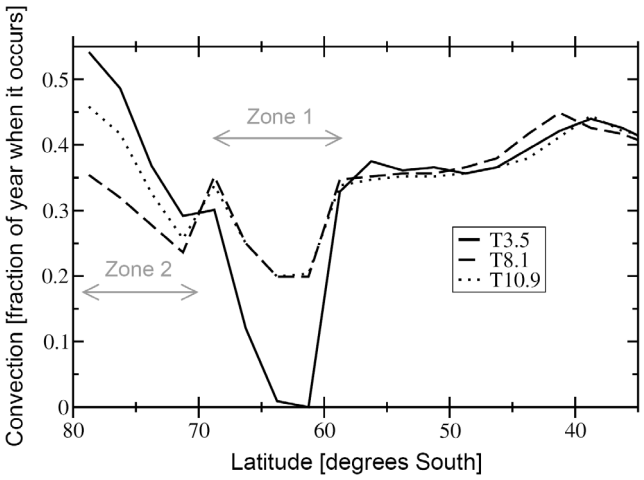

Figure 2. Convection changes in the Southern Ocean for three of the warm climate simulations presented here. Figure 2 presents the fraction of the year in which the surface layer convects with the underlaying layer, averaged over the Atlantic and Pacific sectors of the CLIMBER model. That is, a value of 0.5 indicates that convection occurs half of the year. Two particular zones are defined here and discussed in detail in the text. Zone 1 is the location of maximum sea ice extension, and hence of seasonal sea ice melting, for the T3.5 simulation. Zone 2 is the zone of deep water formation along the Antarctic continent.

three simulations presented there are typical of the three different states we obtain in the warm climate simulation realized. T3.5 is a good example for the behavior of CTRL, T3.5 and T4.6: Because of the presence of sea ice which melts in the region defined as zone 2 in Figure 2 there is no convection around 60° to 65°S (for T3.5), and there is deep convection along the Antarctic continent, favored by the formation of sea ice in zone 2. Therefore the $\delta^{18}O_{sw}$ decreases while the average temperature increases for the CTRL, T3.5 and T4.6 sequences. When the climate warms further, sea ice no longer extends to zone 1, where some convection starts (for T8.1, analog for T7.8 also). The disappearance of sea ice reduces the salinity of waters along the Antarctic continent and slows the deep convection. This change in deep water formation helps the surface $\delta^{18}O_{sw}$ to decrease further as the surface layer is less mixed with the underlaying ocean. Finally, Figure 2 also shows that for T10.9 there is renewed deep oceanic convection along the Antarctic, but this time following a thermal mode, as mentioned before. T10.9 has therefore a convection in this region which resembles more the CTRL, thus the surface $\delta^{18}O_{sw}$ is less negative than for T8.1.

[15] In Figure 1, simulations with major changes in the rate of deep water formation are not presented. In particular, the Northern Hemispheric averages for T3.5 and T7.8 are not shown as they underwent nonnegligible spontaneous intermediate water formation in the northern part of the Pacific ocean, whose effects are discussed hereafter. T7.8 is shown in section 4.2 to highlight the effect of changes in oceanic circulation.

4. Implications for Isotopic Temperatures

4.1. Effect of Temperature Changes

[16] Figure 3 presents the bias, T-T*, plotted with respect to latitude for simulations without major changes in oceanic circulation. That is, we present the error introduced on the calculated isotopic temperature by using the present-day or the constant $\delta^{18}O_{sw}$ latitudinal distribution. In Figure 3a, the bias in the intertropical band shows an underestimation of estimated temperature of between 0.5° and 1.7°C, fairly

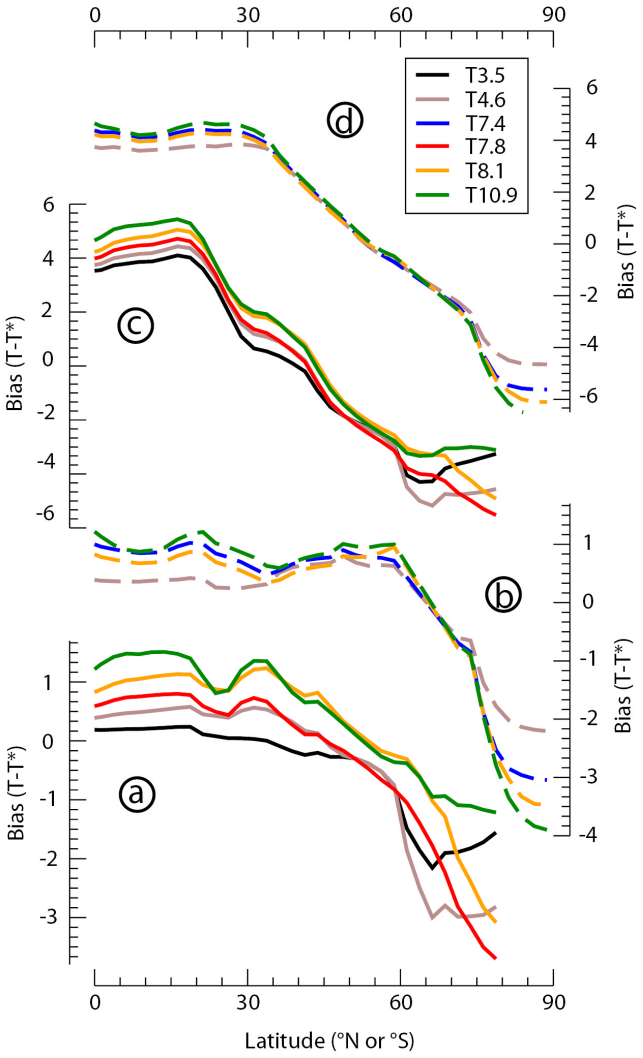

Figure 3. Difference between simulated temperature (T) and simulated isotopic temperature (T*) as a function of latitude at the ocean surface. Solid lines are averages for the Southern Hemisphere; dashed lines are averages for the Northern Hemisphere. Hemispheric averages are taken over the Atlantic and Pacific sectors of the CLIMBER-2 model in each case. (a and b) T* computed using present-day $\delta^{18}O_{sw}$ latitudinal distribution. (c and d) T* computed with $\delta^{18}O_{sw}$ constant for every latitude.

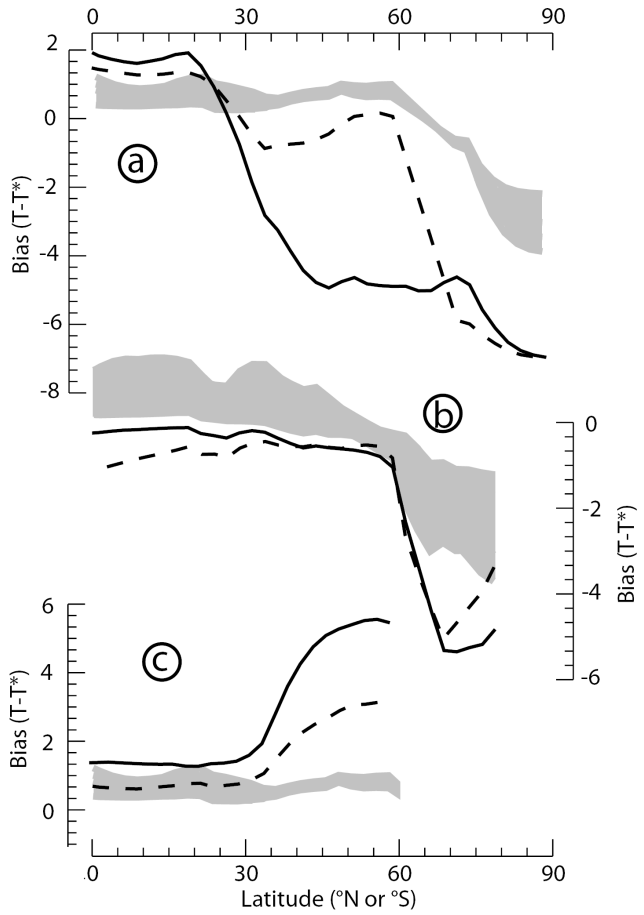

Figure 4. Simulations presenting significant deep oceanic circulation changes: (a) with shutdown of the northern deep water formation, (b) with shutdown of the southern deep water formation, and (c) with initiation of intermediate water formation in the North Pacific. Figure 4a (Figure 4b) is obtained via the addition of a permanent freshwater flux of 1 Sv to the North Atlantic Ocean (Southern Ocean), without $\delta^{18}O_{sw}$ content. Initiation of intermediate water formation in the North Pacific was found to be present spontaneously in simulation T7.8 presented before and is shown here for the Northern Hemisphere. The bias is computed with T* using the present-day $\delta^{18}O_{sw}$ latitudinal profile. For each plot the solid line gives the anomaly for a single basin (northern Atlantic (Figure 4a)), southern Atlantic and Southern Ocean (Figure 4b), and North Pacific (Figure 4c)), and the dashed line shows the equivalent but for hemisphere averages (as in Figure 3). The shaded envelopes mark the range of the bias, T-T*, in the absence of major oceanic circulation reorganization (taken from Figures 3a and 3b).

constant between the equator and 30°S. Therefore the temperature gradient inferred in this region is mostly unaffected; the absolute values are shifted by the bias value. The bias then decreases to zero around 50°S. It should be noted that the warmer the climate, the higher in latitude the bias crosses zero, because of changes in the partitioning of the $\delta^{18}O_{sw}$ following the "compensation effect." That is, the warmer the climate, the more water is transported to high latitudes and the more depleted high-latitude $\delta^{18}O_{sw}$ becomes. The amplitude of the bias then continuously increases toward high latitudes up to 3°C at 80°S. This implies an underestimation of the equator-to-pole estimated temperature gradient by up to 4.7°C. Results are even more dramatic when considering a constant $\delta^{18}O_{sw}$ (Figures 3c and 3d). The bias is, then, considerably larger both at low and high latitudes. The error introduced in the equator-to-pole gradient is up to 8°C. Figures 3b and 3d show that the simulated bias in the Northern Hemisphere is quite consistent with that of the Southern Hemisphere, both at low and high latitudes, reaching 2° to 3.5°C for Figure 3b and 4° to 7°C for Figure 3d. The error introduced in the equator-to-pole gradient is here 5°C for Figure 3b and 10°C for Figure 3d. These are huge differences when comparing to an averaged equator-to-pole gradient of about 30° in the present day.

4.2. Effect of Major Oceanic Circulation Changes

[17] Figure 4 presents the results of simulations where major oceanic deep circulation changes occurred. Three different simulations are presented to highlight classical circulation changes, which we know have occurred in the past: shutdown of the northern bottom water formation (Figure 4a); start of intermediate waters formation in the northern Pacific (Figure 4c) and disruption of the Antarctic bottom water formation (Figure 4b). These simulations are shown to provide insight on the effect of major circulation reorganization on surface $\delta^{18}O_{sw}$; they have to be understood as an indication of the bias introduced when considering other climates with different oceanic circulation [*Brass et al.*, 1982; *Barrera et al.*, 1997; *Thomas*, 2004]. Neglecting the northern or southern disruption of deep waters formation leads to an additional major temperature overestimation, up to 2°C (around 70°S, Figure 4b) and up to 5°C (around 50°N, Figure 4a). The anomaly is not confined to high latitudes, but extends southward to 30°N (Figure 4a). Conversely, the simulation of an active intermediate water formation in the northern Pacific Ocean (e.g., as suggested for the Eocene [*Thomas*, 2004] or for the latest Cretaceous [*Barrera and Savin*, 1999; *Frank et al.*, 2005]) leads to an opposite bias (that is an underestimation) from 2° to 5.5°C, depending on latitude. This is because the formation of intermediate waters helps to mix high-latitude low $\delta^{18}O_{sw}$ and therefore comparatively enhances the $\delta^{18}O_{sw}$ of surface water. Figure 4 therefore emphasizes that changes in oceanic circulation have a major impact on the surface $\delta^{18}O_{sw}$ content of the oceans and therefore on temperature estimations derived from $\delta^{18}O_{Ca}$. They should by no means be neglected.

4.3. An Outlook Toward Data

[18] In order to show the implications of our results with respect to data-derived latitudinal gradients, we define a new isotopic temperature, T°. It is based on the same formula as T*, but in which the $\delta^{18}O_{Ca}$ term is the measured isotopic content of the calcite, obtained from data (see Figure 5). To compute T° we also need an assumption on the $\delta^{18}O_{sw}$ content of surface waters. It is taken to be either constant to −1‰ (for an "ice-free" world [*Shackleton and*

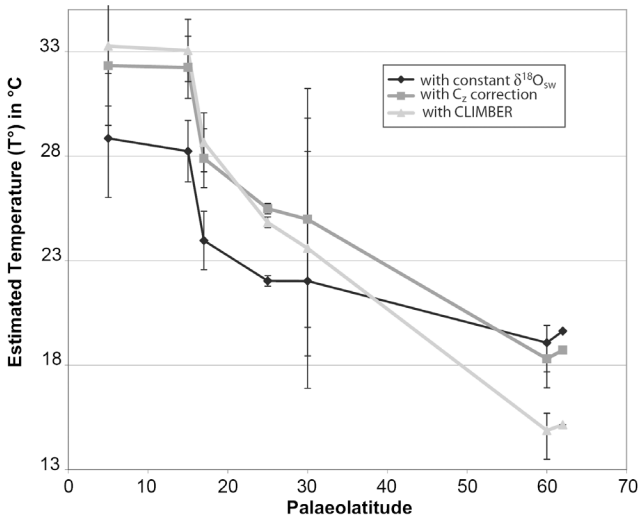

Figure 5. Impact of $\delta^{18}O_{sw}$ changes on data-derived isotopic temperature for the Cenomanian-Turonian interval, plotted as T°. Data in oxygen isotopic content of calcite are taken from [*Bice and Norris*, 2002] and then interpreted in terms of estimated temperature, T° (see text), following three assumptions for the $\delta^{18}O_{sw}$. The solid line shows T° calculated with a constant −1‰ latitudinal content, the dark shaded line shows T° calculated with a present-day latitudinal content (C_z correction, see section 4.3), the light shaded line shows T° calculated with the C_c correction calculated from the T7.4 simulation with the CLIMBER-2 model. Squares, triangles, and diamonds show the mean of all data points at given latitudes; thin vertical black bars show the range of all points. The effect of the successive corrections is to increase the latitudinal temperature gradient. Taking into account the correction from the CLIMBER-2 model leads to a latitudinal temperature gradient more compatible with model simulations of past warm climates.

Kennett, 1975]) or equal to the formula below [*Zachos and Stott*, 1994], specifically established for the present-day Southern Hemisphere:

$$C_z = 0.576 + 0.041L - 0.0017L^2 + 1.35 * 10^{-5}L^3 \quad (4)$$

where L is the latitude in degrees south. A third assumption is to use C_z, and to add a correction computed with the CLIMBER-2 model, as

$$C_c = \delta^{18}O_{sw}(t_w) - \delta^{18}O_{sw}(t_R) \quad (5)$$

where $\delta^{18}O(t_w)$ (respectively $\delta^{18}O_{sw}(t_R)$) represents the $\delta^{18}O_{sw}$ simulated in the warm (respectively reference) climate state. Our results show that, in contrast with what was commonly assumed, the evolution of the surface $\delta^{18}O_{sw}$ of surface water in warm climates would tend to underestimate (respectively overestimate) the isotopic temperature in the intertropical band (respectively at high latitudes) if the present-day $\delta^{18}O_{sw}$ profile, or a latitudinally constant one, is assumed. The systematic bias arising from this common hypothesis is large, especially if one neglects changes in oceanic circulation. Simulations including 18O could prove useful to interpret peculiar isotopic data [*Bice et al.*, 2003] for periods in which the oceanic circulation is likely to have been quite different from the modern one. Our work therefore provides new insights that may help to elucidate the issue raised by the weaker-than-modern meridional temperature gradient inferred for past warm climates. We show that inappropriate assumptions on the surface water $\delta^{18}O_{sw}$ in the past, as shown on Figure 4, are likely to contribute to flatten the latitudinal sea surface temperature gradients calculated from calcite or apatite $\delta^{18}O$. From Figure 5, it is clear that the two assumptions commonly used as a bracketing (extreme) interval for $\delta^{18}O_{sw}$ (constant $\delta^{18}O_{sw}$ with respect to latitude and present-day latitudinal $\delta^{18}O_{sw}$) yield an underestimation of the latitudinal sea surface temperature gradient when accounting for a full modeling of ^{18}O changes both in the ocean and atmosphere and not only for $\delta^{18}O_p$. A more adequate correction would require a model configuration including changes in geography for specific greenhouse episodes.

5. Conclusions

[19] With the present study we demonstrate that the evolution of surface waters $\delta^{18}O$ content in warm climates is such that common assumptions tend to underestimate the inferred latitudinal isotopic temperature gradient. We showed that this is an effect of changed atmospheric water transport and changed global partitioning of the oxygen 18 isotopes in the ocean. The partitioning is modified in warm climates between high-latitude surface and deep oceanic waters on the one hand and surface and intermediate intertropical waters on the other hand. This evolution is named the "compensation effect" here to highlight its potential in compensating the changes in isotopic composition of precipitation that occurred at the same time. Results from a set of warm climate experiments indicate that taking into account the evolution of the $\delta^{18}O$ of surface water could help elucidate part of the weaker-than-modern sea surface temperature gradient issue in warm climates. We emphasize here that our results are particularly relevant for the calculation of high-latitude isotopic temperatures, as these regions are the most largely affected by the modeled changes in $\delta^{18}O_{sw}$. The new step provided here, accounting for ocean circulation response, opens wide perspectives for understanding warm climates of the earth. Doing so will help reduce data-model discrepancies without requiring considerable changes in latitudinal heat transport which climate models cannot produce.

[20] **Acknowledgments.** We are grateful to G. Ramstein for constructive comments on the manuscript. We also thank P. Ward for proofreading the manuscript and two anonymous reviewers for fruitful reviews.

References

Barrera, E., and S. Savin (1999), Evolution of late Campanian-Maastrichtian marine climates and oceans, *Spec. Pap. Geol. Soc. Am.*, *332*, 245–282.

Barrera, E., S. Savin, E. Thomas, and C. Jones (1997), Evidence for thermohaline circulation reversals controlled by sea-level change in the latest Cretaceous, *Geology*, *25*, 715–718.

Bice, K., and R. Norris (2002), Possible atmospheric CO_2 extremes of the Middle Cretaceous (late Albian–Turonian), *Paleoceanography*, *17*(4), 1070, doi:10.1029/2002PA000778.

Bice, K., B. Huber, and R. Norris (2003), Extreme polar warmth during the Cretaceous greenhouse? Paradox of the late Turonian $\delta^{18}O$ record at Deep Sea Drilling Project Site 511, *Paleoceanography*, *18*(2), 1031, doi:10.1029/2002PA000848.

Brass, G., J. Southam, and W. Peterson (1982), Warm saline bottom water in the ancient ocean, *Nature*, *269*, 620–623.

Crowley, T., and J. Zachos (2000), *Warm Climates in Earth History*, pp. 50–76, Cambridge Univ. Press, New York.

Delaygue, G., J. Jouzel, and J.-C. Dutay (2000), Oxygen-18 salinity relationship simulated by an oceanic general circulation model, *Earth Planet. Sci. Lett.*, *178*, 113–123.

Ditchfield, P., J. Marshall, and D. Pirrie (1994), High latitudes paleotemperatures variations: New data from the Tithonian to Eocene of James Ross Island, *Palaeogeogr. Palaeoclimatol. Palaeoecol.*, *107*, 70–101.

Epstein, S., R. Buchsbaum, H. Lowenstam, and H. Urey (1953), Revised carbonate–water isotopic temperature scale, *Geol. Soc. Am. Bull.*, *64*, 1315–1326.

Erez, J., and B. Luz (1983), Experimental paleotemperature equation for planktonic foraminifera, *Geochim. Cosmochim. Acta*, *47*, 1025–1031.

Frank, T. D., D. Thomas, R. M. Leckie, M. A. Arthur, P. R. Bown, K. Jones, and J. A. Lees (2005), The Maastrichtian record from Shatsky Rise (northwest Pacific): A tropical perspective on global ecological and oceanographic changes, *Paleoceanography*, *20*, PA1008, doi:10.1029/2004PA001052.

Huber, B., D. Hodell, and C. Hamilton (1995), Middle-Late Cretaceous climate of the southern high latitudes: Stable isotopic evidence for minimal equator-to-pole thermal gradients, *Geol. Soc. Am. Bull.*, *107*, 1164–1191.

Huber, B. T., R. D. Norris, and K. G. MacLeod (2002), Deep-sea paleotemperature record of extreme warmth during the Cretaceous, *Geology*, *30*, 123–126.

Huber, M., and L. C. Sloan (1999), Warm climate transitions: A general circulation modeling study of the late Paleocene thermal maximum (~56 Ma), *J. Geophys. Res.*, *104*, 16,633–16,656.

Huber, M., and L. Sloan (2001), Heat transport, deep waters, and thermal gradients: Coupled simulation of an Eocene greenhouse climate, *Geophys. Res. Lett.*, *28*, 3481–3484.

Jouzel, J., G. Hoffmann, R. Koster, and V. Masson (2000), Water isotopes in precipitation: Data/model comparison for present-day and past climates, *Quat. Sci. Rev.*, *19*, 363–379.

Kiehl, J., and R. E. Dickinson (1987), A study of the radiative effects of enhanced atmospheric CO_2 and CH_4 on early Earth surface temperatures, *J. Geophys. Res.*, *92*, 2991–2998.

Manabe, S. (1997), Early development in the study of greenhouse warming: The emergence of climate models, *Ambio*, *26*(1), 47–51.

Norris, R. D., K. Bice, E. Mango, and P. Wilson (2002), Jiggling the tropical thermostat during the Cenomanian ''hothouse'', *Geology*, *30*, 299–302.

Paren, J., and J. Potter (1984), Isotopic tracers in polar seas and glacier ice, *J. Geophys. Res.*, *89*, 749–750.

Pearson, P., P. W. Ditchfield, J. Singano, K. G. Harcourt-Brown, C. Nicholas, R. K. Olsson, N. Shackleton, and M. A. Hall (2001), Warm tropical sea surface temperatures in the Late Cretaceous and Eocene epochs, *Nature*, *413*, 481–487.

Petoukhov, V., A. Ganopolski, V. Brovkin, M. Claussen, A. Eliseev, C. Kubatzki, and S. Rahmstorf (2000), CLIMBER-2: A climate system model of intermediate complexity. part I: Model description and performance for present climate, *Clim. Dyn.*, *16*, 1–17.

Pierrehumbert, R. (2002), The hydrologic cycle in deep-time climate problems, *Nature*, *419*, 191–198.

Pirrie, D., and J. Marshall (1990), High-paleolatitude Late Cretaceous paleotemperatures: New data from James Ross Island, Antarctica, *Geology*, *18*, 31–34.

Pucéat, E., C. Lécuyer, S. M. F. Sheppard, G. Dromart, S. Reboulet, and P. Grandjean (2003), Thermal evolution of Cretaceous Tethyan marine waters inferred from oxygen isotope composition of fish tooth enamels, *Paleoceanography*, *18*(2), 1029, doi:10.1029/2002PA000823.

Roche, D., D. Paillard, A. Ganopolski, and G. Hoffmann (2004), Oceanic oxygen-18 at the present day and LGM: Equilibrium simulations with a coupled climate model of intermediate complexity, *Earth Planet. Sci. Lett.*, *218*, 317–330.

Sellwood, B., G. Price, and P. Valdes (1994), Cooler estimates of Cretaceous temperatures, *Nature*, *370*, 453–455.

Shackleton, N. (1974), Attainment of isotopic equilibrium between ocean water and the benthonic foraminifera genus *Uvigerina*: Isotopic changes in the ocean during the last glacial, in *Les méthodes quantitatives d'étude des variations du climat au cours du pléistocène*, pp. 203–210, Cent. Natl. de la Rech. Sci., Gif-sur-Yvette.

Shackleton, N., and J. Kennett (1975), Paleotemperature history of the Cenozoic and the initiation of Antarctic glaciation: Oxygen and carbon isotope analyses in DSDP Sites 277, 279 and 281, *Initial Rep. Deep Sea Drill. Proj.*, *29*, 743–755.

Sloan, L. C., J. C. G. Walker, and T. C. Moore Jr. (1995), Possible role of oceanic heat transport in early Eocene climate, *Paleoceanography*, *10*, 347–356.

Thomas, D. (2004), Evidence for deep-water production in the North Pacific Ocean during the early Cenozoic warm interval, *Nature*, *430*, 65–68.

Wilson, P. A., and R. D. Norris (2001), Warm tropical ocean surface and global anoxia during the mid-Cretaceous period, *Nature*, *412*, 425–428.

Wilson, P. A., R. D. Norris, and M. J. Cooper (2002), Testing the mid-Cretaceous ''greenhouse hypothesis'' using Turonian pristine foraminiferal calcite from Demerara Rise, *Geology*, *30*, 607–610.

Zachos, J., and L. Stott (1994), Evolution of early cenozoic marine temperatures, *Paleoceanography*, *9*, 353–387.

Y. Donnadieu, D. Paillard, E. Pucéat, and D. M. Roche, Laboratoire des Sciences du Climat et de l'Environnement, CEA-CNRS, Orme des Merisiers, F-91191 Gif-sur-Yvette Cedex, France. (droche@cea.fr)